Supplementary Data

Probing for DNA damage with β-hairpins: Similarities in incision efficiencies of bulky DNA adducts by prokaryotic and human nucleotide excision repair systems *in vitro*.

Yang Liu[a], Dara Reeves[a], Konstantin Kropachev[a], Yuqin Cai[b], Shuang Ding[b], Marina Kolbanovskiy[a], Alexander Kolbanovskiy[a], Judith L. Bolton[c], Suse Broyde[b], Bennett Van Houten[d], and Nicholas E. Geacintov[a,*]

[a]Chemistry and [b]Biology Departments, New York University, 31 Washington Pl., New York, NY 10003; [c]Department of Medicinal Chemistry and Pharmacognosy, College of Pharmacy, University of Illinois at Chicago, Chicago, IL 60612, and [d]Department of Pharmacology and Chemical Biology, University of Pittsburgh School of Medicine, Pittsburgh, PA 15213, USA

11-mers

GGTA*GCG*ATGG (VI)

GGTA*GAG*ATGG (VII)

135-mer duplex VI

5' 62-mer | 11-mer |3' 62-mer

5'GACCTGAACACGTACGGAATTCGATATCCTCGAGCCAGATCTGCGCCAGCTGGCCACCCTGA*GGTAGCGATGG*GAGCG

CCAAGCTTGGGCTGCAGCAGGTCGACTCTAGAGGATCCCGGGCGAGCTCGAATTCGC3'

135-mer duplex VII

5' 62-mer | 11-mer |3' 62-mer

5'GACCTGAACACGTACGGAATTCGATATCCTCGAGCCAGATCTGCGCCAGCTGGCCACCCTGA*GGTAGAGATGG*GAGCG

CCAAGCTTGGGCTGCAGCAGGTCGACTCTAGAGGATCCCGGGCGAGCTCGAATTCGC3'

Scheme I. Sequences of 135-mer duplexes VI and VII (Figure 8). In the cases of the experiments depicted in Figure 4, the underlined portions were replaced by sequence I shown in Figure 2 (5'-CCATCG$_6$CTACC) for the studies with *cis*- and *trans*-BP-dG$_6$ adducts .

5’-^{32}PGAC TAC GTA CTG **TCA CAX G*XA CAC** GCT ATC TGG CCA GAT CCG C-3’
3’-CTG ATG CAT GAC AGT GT Y C YT GTG CGA TAG ACC GGT CTA GGCG-5’

43-mer duplexes (Figure 5B). The sequence colored in red is IV and V in Figure 2 of the main text (X = C, or T, and Y is G or A, respectively).

5′-^{32}PGACTACGTACTGT**CCATC$_5$GC$_7$TACC**GCTATCTGGCCAGATCCGC-3′
3′-CTGATGCATGACAGGTAG C G ATGGCGATAGACCGGTCTAGGCG-5′

43-mer duplexes (Figure 7, 4-OHEN-dC adducts)). The sequence colored in red is I in Figure 2 (main text)

5’-^{32}PGACTACGTACTGTTACGGCTGAGC**ATGCG$_6$G$_7$CCTAC**GCAATCAGGCCAGATCTGC-3’
3’ CTGATGCATGACAATGCCGACTC GTACG C C GGATGCGTTAGTCCGGTCTAGACG-5’

54-mer duplexes (Figures 5C and 6; *trans*-BP-dG adducts). The sequence colored in red is sequence V In Figure 2 of the main text. Sequence I (5’-**CCATCG$_6$CTACC**) was substituted for V in the experiments with *trans*-BP-dG –I duplexes described in Figure 5C.

Scheme 2. Sequences of 43-mer and 54-mer duplexes.

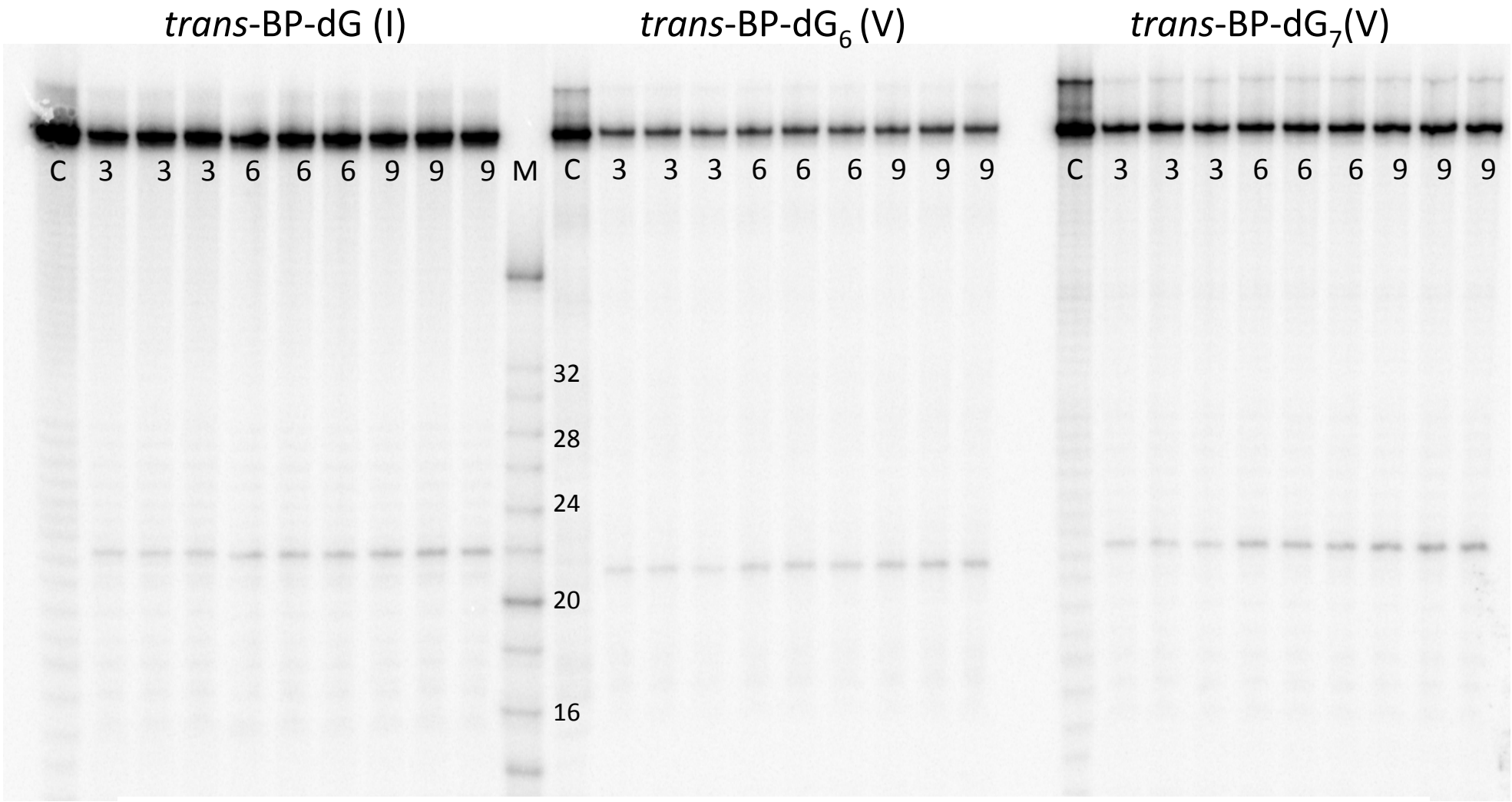

Figure S1A. Typical gel autoradiograms of experiments depicting incisions catalyzed by UvrABC^{Bca} at 55 ^{0}C at different incubation time points of 3, 6, or 9 min, as indicated. Each identical sample was loaded three times to verify the reproducibility (these are not considered as independent experiments). C: Controls; M:size markers. The 54 nt long oligonucleotides were 5'-endlabeled, yielding 22 nt incision products in the case of *trans*-BP-dG duplexes I and –dG$_7$(V), and 21 nt in the case of –dG$_6$ (V).

Gel 050807 Bca55

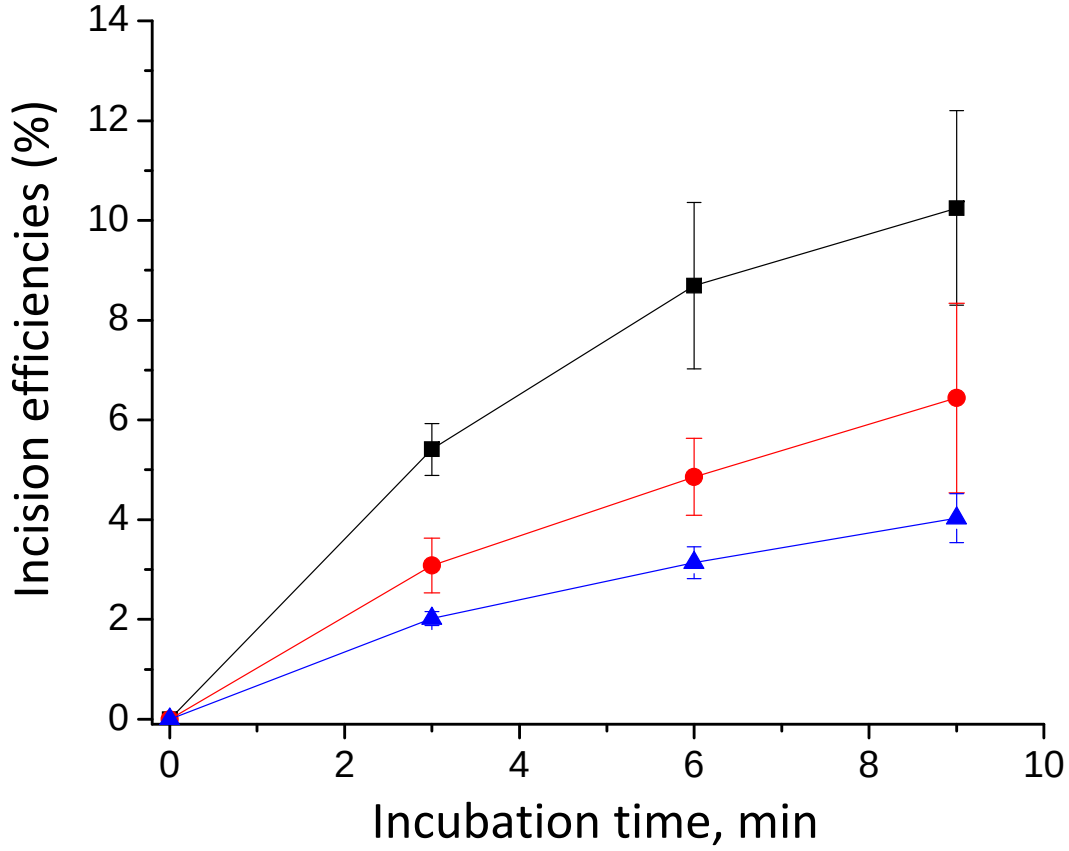

Figure S1B. Incision kinetics of *trans*-BP-dG (I) (blue), *trans*-BP-dG$_7$ (V) (red), and *trans*-BP-dG$_7$ (V) (black), catalyzed by UvrABC^{Bca} at 55 ^{0}C as shown in Figure S1A. Averages and standard deviations are for four sets of independent experiments. The 3 min time points were used in the bar graph in Figure 5C of the main text.

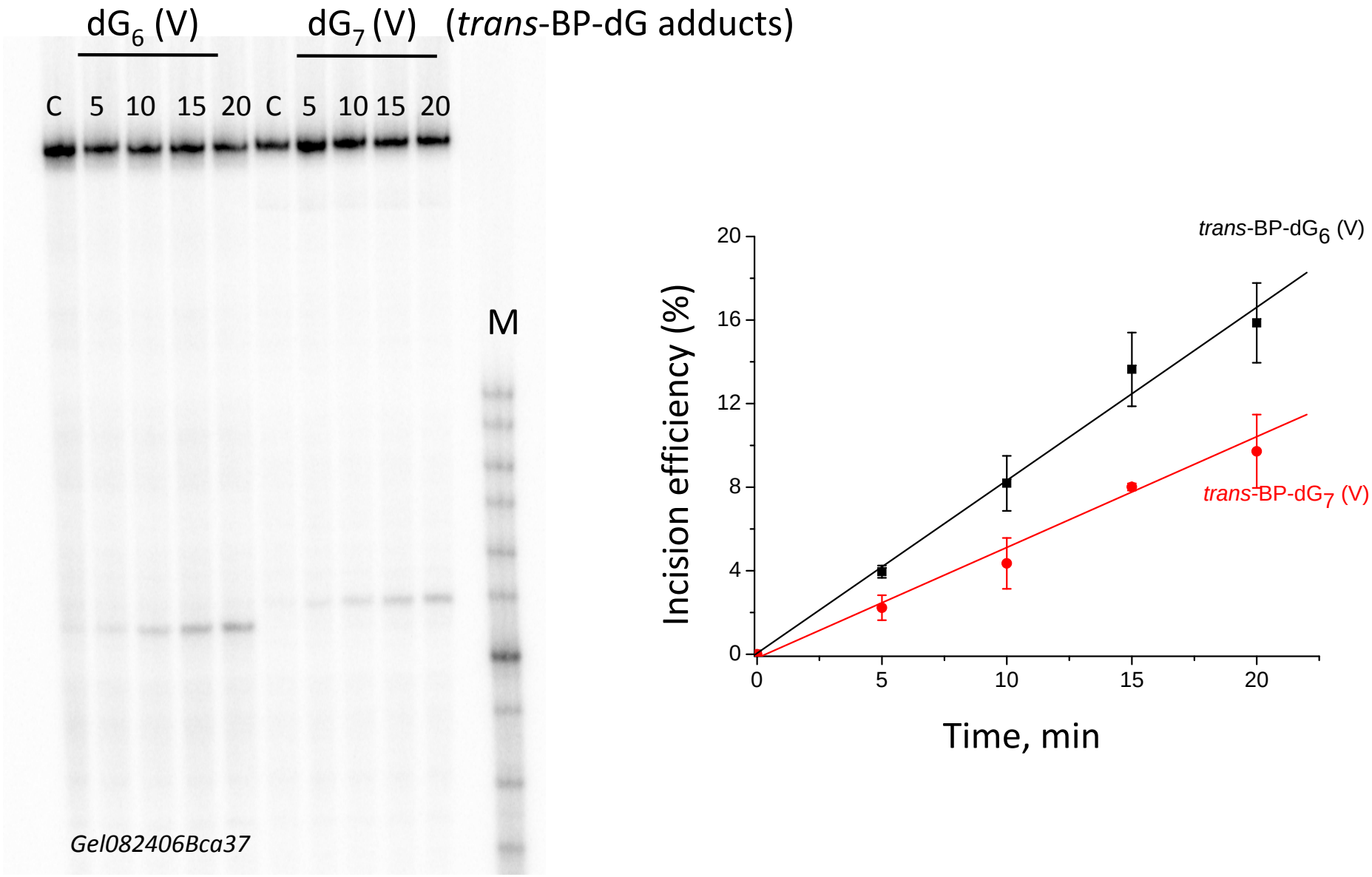

Figure S2. Typical gel autoradiograms of experiments depicting incisions catalyzed by UvrABC^{Bca} at 37 ^{0}C at different incubation time points indicated (min). C: controls, M: markers. (Left). Incision kinetics depicting averages and standard deviations from eight independent experiments (right). The straight lines are the best linear fits to the data points. Experiments were conducted with 5'-end labeled 54-mer oligonucleotides.

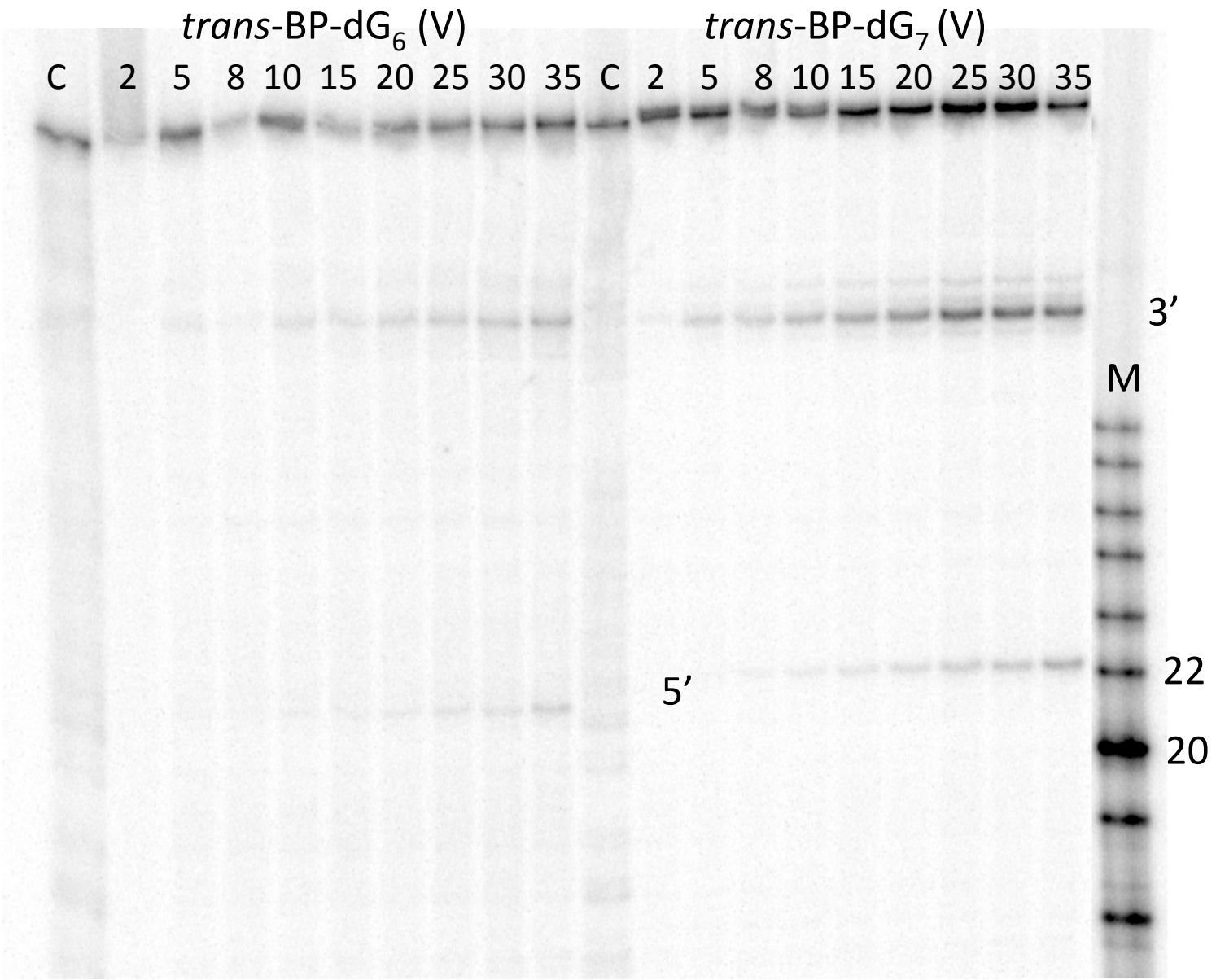

Figure S3A. Kinetics of incisions catalyzed by UvrABC^{Cho} at 37 ^{0}C. C: Controls, M:markers. The 3’-Cho incision products are indicated (38-mers, markers not shown). The indicated 5’-incisions are attributed to traces of *E.coli* UvrC in these preparations.

Gel022206Cho37

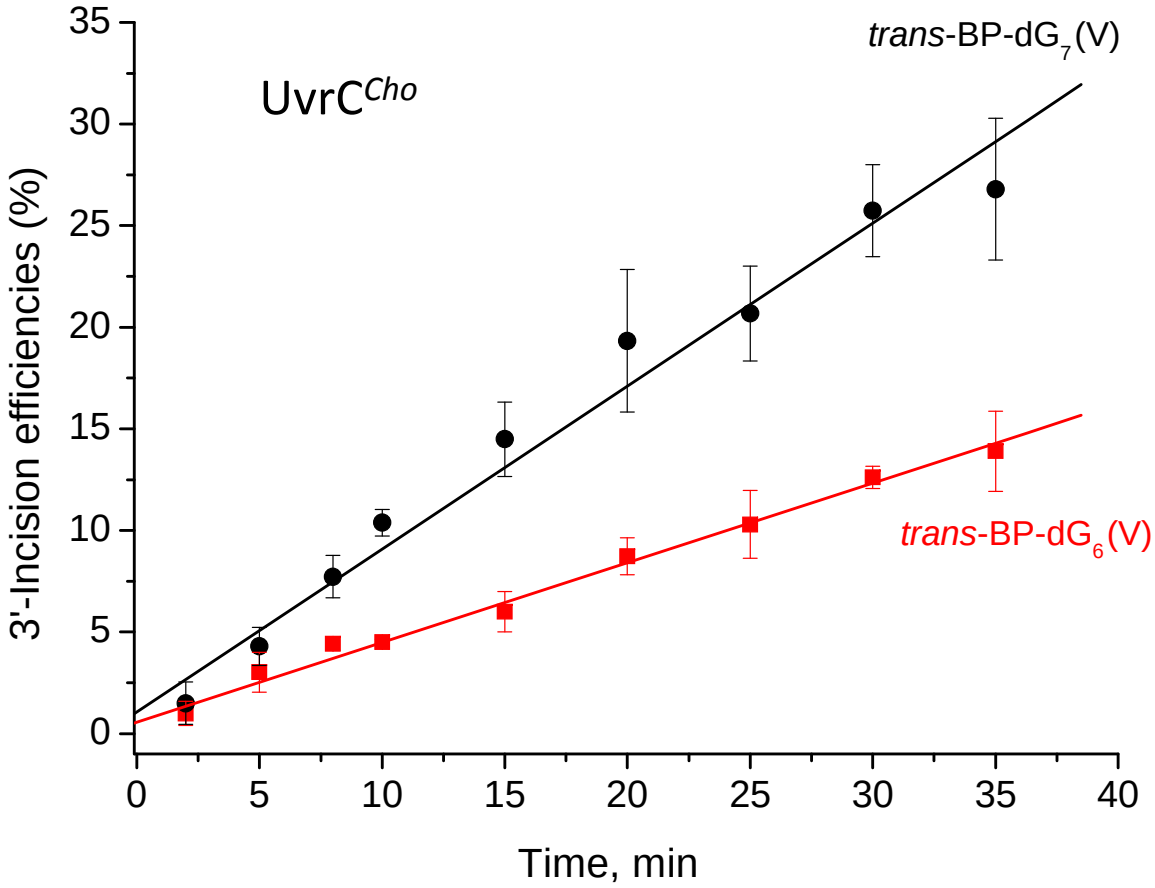

Figure S3B. Incision kinetics of duplexes V containing either the *trans*-BP-dG_6 or $-dG_7$ lesion by UvrABC^{Cho} (UvrcA and UvrB were from *Bca*). The data points are averages and standard deviations from three independent experiments ; the lines are the best linear fits to the data points. Experiments were conducted with 5'-end labeled 54-mer oligonucleotides at 37 ^{0}C.

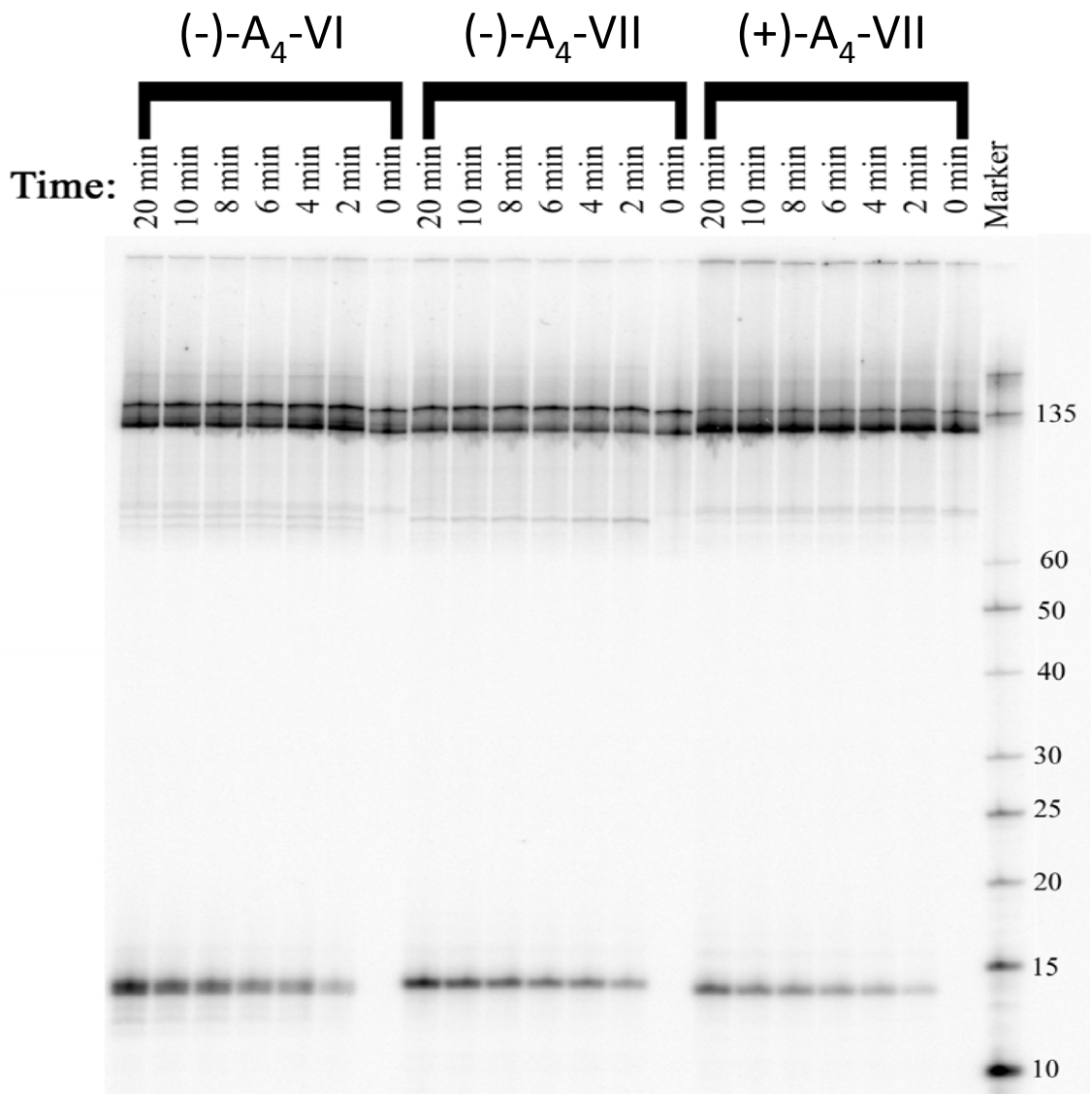

Figure S4A. Example of an autoradiogram of relative NER incision efficiencies of different stereoisomeric 4-OHEN-dA adducts in sequence contexts VI or VII embedded in the middle of internally labeled 135-mer DNA duplexes catalyzed by UvrABC*Tma* proteins at 55 ^{0}C.

Gel082609

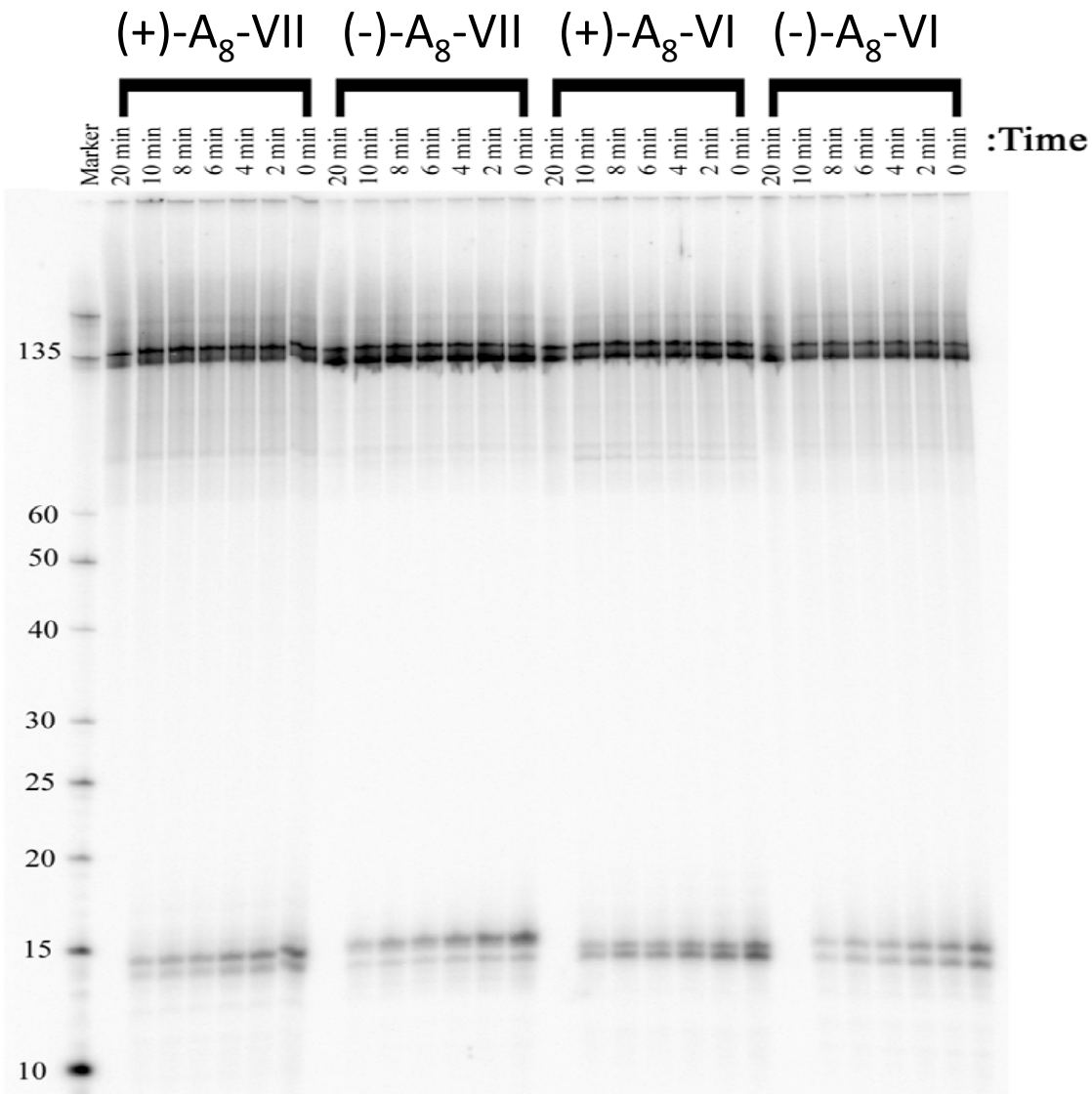

Figure S4B. Example of an autoradiogram of relative NER incision efficiencies of different stereoisomeric 4-OHEN-dA adducts in sequence contexts VI or VII embedded in the middle of internally labeled 135-mer DNA duplexes catalyzed by UvrABC*Tma* proteins at 55 ^{0}C.

Gel081509

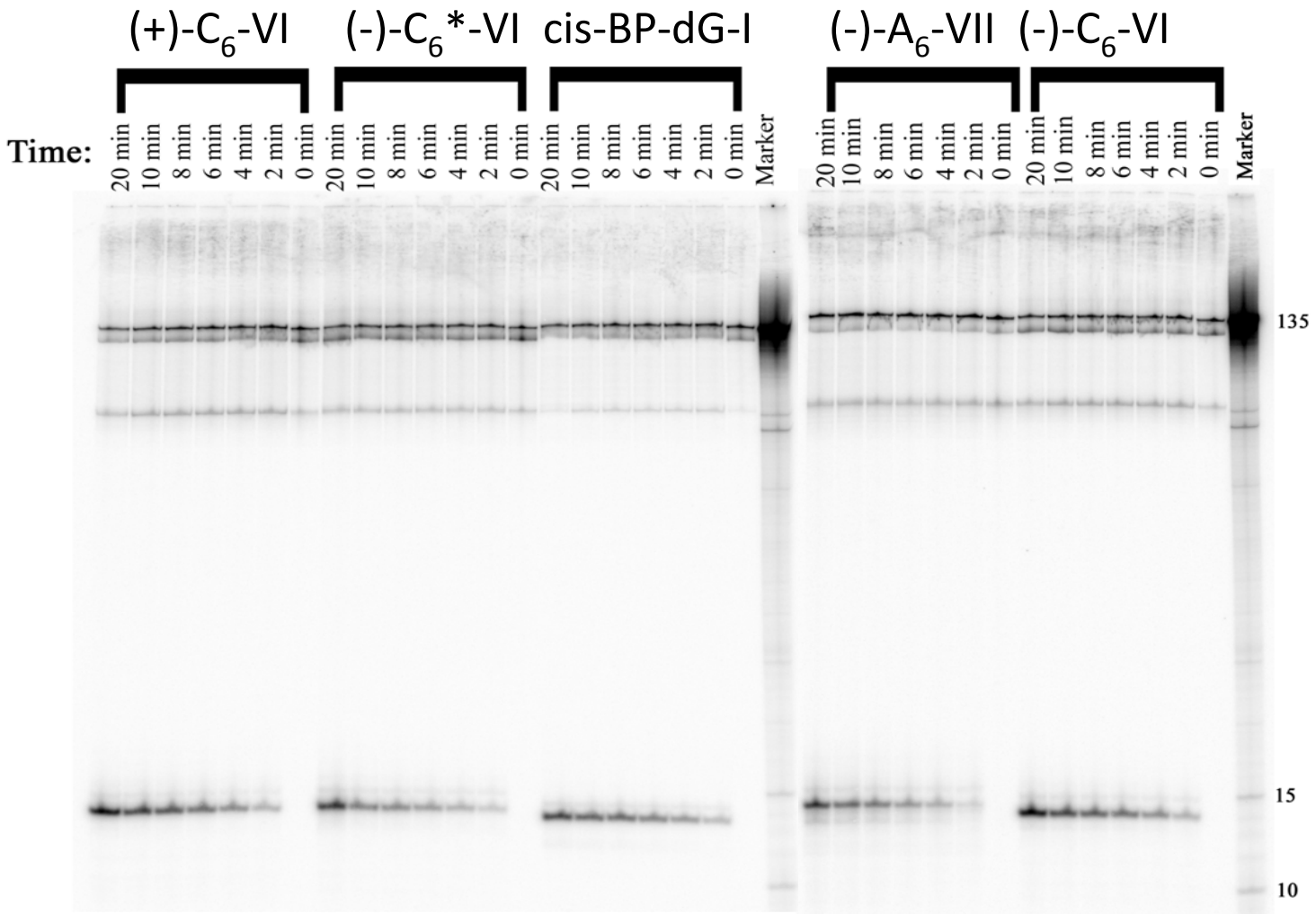

Figure S4C. Example of an autoradiogram of relative NER incision efficiencies of different stereoisomeric 4-OHEN-dA and –dC adducts in sequence contexts VI or VII embedded in the middle of internally labeled 135-mer DNA duplexes catalyzed by UvrABC^{Tma} proteins at 55 ^{0}C. The (-)-C_6*-VI adduct is a minor 4-OHEN-dC adduct (isomer C^2, Kolbanovskiy et al., *Chem Res Toxicol.* 2005 Nov;18(11):1737-47 cited in the main text) which was not investigated in detail here. The results with the *cis*-BP-dG adduct indicate that the incision efficiencies of the 4-OHEN-dC/dA adducts are not radically different.